Design of Electromagnetic Acoustic Transducer for Helical Lamb Wave with Concentrated Beam

Zhe Wang, Songling Huang, *Senior Member, IEEE*, Shen Wang, Qing Wang, *Senior Member, IEEE*, and Wei Zhao

***Abstract*—Guided wave is advantageous to inspect pipe-like structures because of its long-distance propagation. Due to the curved structure of pipeline, guided wave can spread spirally with a helix angle. However, the current transducers focus more on the narrow or omni-directional beam than the helical form. This work presents the designed transducer to generate helical Lamb wave with concentrated beam. The transducer is developed using permanent magnets and arc-coil based on the principle of electromagnetic-acoustic conversion. The numerical analysis applying finite element method is conducted to verify the theoretical model of the transducer. The angular profiles are obtained to study the propagation of helical Lamb wave. Further, experiments are designed to demonstrate the performance of proposed transducer. The results from the experiments show good agreement with the numerical simulations. Besides, the parameter of central width is investigated and the half-angle of divergence is calculated. The results are compared with that from traditional transducers. The comparison indicates the superiority of the proposed transducer in generating helical Lamb wave. Therefore, the designed transducer could be a potential alternation for pipeline inspection based on guided wave.**

***Index Terms*—Guided wave, half-angle of divergence, helix angle, pipeline inspection, transducer.**

I. Introduction

THE pipe-like structures have been extensively applied in energy transportation, such as petroleum and natural gas pipeline [1]-[3]. During the long-term service and rough working conditions, the structural fatigue may develop into defects and lead to dangerous situation [4]. The nondestructive evaluation provides multiple methods for pipeline inspection. The magnetic flux leakage and eddy current testing need to use sensors to move along the structure to accomplish the scanning. The radiographic testing is inefficient and it need expensive equipment. However, the ultrasonic guided waves have presented great potential for defect inspection among the detection methods [5]–[8].

Guided wave can propagate along the structure for long distance [9]. The guided wave transmitter and receiver can be placed in the two ends of pipeline to accomplish the inspection [10]. Thus, guided wave is capable to detect the inaccessible locations. Two types of transducers are applied to generate guided wave. The first type is the piezoelectric transducer which utilizes the piezoelectric effect [11]. It needs to be bonded tightly on the surface of inspected object. The second type is the electromagnetic acoustic transducer (EMAT) [12]. It has the advantage of non-contact and can be used in special cases, such as high temperature environment [13]. The EMAT also requires less condition to the cleanliness of pipeline surface than the piezoelectric transducer [14].

Because of the particular structure of pipeline, guided wave could spread in the axial, circumferential and helical directions [15], [16]. The longitudinal and torsional modes propagate axially along the pipeline and they are sensitive to circumferential flaws [17]. The transducer using magnetostrictive effect to generate longitudinal mode had been developed based on coil and bias magnet [18]. Zenghua Liu et al. designed multisplitting meander coil to enhance the signal of corresponding guided wave mode [19]. For torsional modes, Seung Hyun Cho et al. employed transducers using magnetostrictive nickel strip instead of magnet [20]. A configuration of EMAT using a periodic permanent magnet (PPM) was proposed to generate fundamental torsional mode and higher modes [21]. The circumferential guided wave is also available but the transducer must move along the pipeline to finish the detection of pipeline with a certain length [22].

The helical guided wave can propagate along a spiral path between two parallel circumferentially placed transducers [23], [24]. Compared with the guided wave propagating along the axial direction of pipeline, the helical guided wave can pass through the detection area from more spiral angles. Therefore, it is possible to obtain more information about the corresponding defect, which is helpful in constructing a more accurate defect image [25]. Hoe Woong Kim et al. proposed the transducer arrays with segmented magnetostrictive patches to generate helical shear-horizontal wave [26]. The wave can identify defect locations in axial and circumferential directions simultaneously. Besides, they also designed magnetostrictive transducers with a figure-of-eight coil to focus more beam energy along the circumferential direction [17]. However, the current transducers are either concentrated in one direction with narrow beam, or nearly omni-directional which is not favorable to generate helical guided wave in a certain range of angles. In addition, the helical Lamb wave needs more efforts to explore its feasibility. In this work, a helical Lamb wave transducer based on mechanism of Lorentz force is proposed to generate guided wave with beam energy concentrated in certain angles. The transducer is composed of permanent magnets, arc-coil and pipeline itself. The parameters of coil are deliberately designed to match the guided wave and control the wave mode. The characteristics analysis of transducer is employed by simulations and experiments. The objective of the present

research is to promote the study and further application of helical Lamb wave.

The remainder of this article is organized as follows. Section II presents the developed transducer and corresponding principles for generating helical Lamb wave. In section III, the theoretical model is constructed to analyze the transduction process in the EMAT. The numerical simulation is conducted to validate the effectiveness of this transducer in Section IV. Section V is devoted to the experimental analysis. The half angle of divergence is adopted to measure the performance and the results are compared with those from traditional transducers. Concluding remarks and future work are given in Section VI.

II. PROPOSED EMAT

The EMAT utilizes the electromagnetic field to generate the acoustic field in solid plate or pipeline. Fig. 1 presents the configuration of the developed EMAT. This EMAT consists of three components: the arc-coil, the permanent magnets and pipeline itself. The coil is made by flexible printed circuit board (PCB) technology so that it can be bonded around the pipeline surface tightly. The high power pulse with a certain time duration flows into the coil. The windowed tone-burst is used as the pulse and its expression is given by

$$P(t) = w(t) \cdot \sin(2\pi f_c t) \tag{1}$$

where *P(t)* is the pulse, *fc* is the frequency, and *w(t)* is the window function. The Hamming function is applied as the window and it owns the form of

$$w(t) = 0.54 - 0.46 \cdot \cos(2\pi t/T) \tag{2}$$

where *T* is the time duration. Actually, the pulse is windowed sinusoidal signal to improve the spectrum characteristic.

The permanent magnets are utilized to provide bias magnetic field. After the interaction of the electromagnetic field and eddy current, the vibration will occur in the pipeline and form guided wave. The theoretical model for generating helical Lamb wave is explained in next section.

To enhance the ultrasonic signal, the parameters of arc-coil are deliberately designed. The principle of wave superposition is adopted and the distances in the inner of coil are related to wavelength which is denoted as λ. The arc length in the center part called central width is denoted as w_c. To better figure out the superposition of guided wave, Fig. 2 is presented. The pipeline structure is expanded into a flat plate to indicate the distance relation clearly.

The arc-coil in the developed transducer can be divided into four coil-clusters which play important roles to generate helical Lamb wave. The four coil-clusters can be regarded as sectors and own the same center which is denoted as O. The radii of the coil-clusters are denoted as r_1, r_2, r_3 *and* r_4, respectively. For one point in pipeline surface which is denoted as *P*, the distance between this selected point and the center is denoted as r_p. When the waves from the coil-clusters arrive the point *P*, the total fluctuation is the summation of vibrations from four coil-clusters according to the wave superposition. The phases of vibrations from each coil-cluster can be expressed as

$$\varphi_i = \frac{2\pi(r_p - r_i)}{\lambda} - \omega t + \phi_i, \quad i = 1, 2, 3, 4 \tag{3}$$

where ϕ_i is the initial phase of each coil-cluster. The flow direction of current brings the difference of initial phase. If the current directions of two coil-clusters are the opposite to each other, the phase difference will be π. To achieve the effect of wave magnitude superposition, the phase difference in point *P* from two coil-clusters must satisfy

$$\Delta\varphi = \varphi_i - \varphi_j = 2n\pi \quad i \neq j,\ n = 0, 1, 2, \cdots \tag{4}$$

where Δ_φ is the phase difference and n is the non-negative integer. According to the aforementioned principle, the distances between the coil-clusters are obtained. As the results shown in Fig. 1, the distances are the odd or even number of times of half-wavelength.

The velocity of guided wave is usually the input parameter to determine the defect location even the imaging. For helical guided wave, when the thickness of pipeline is far less than its diameter, the guided wave can be considered as the plate-wave propagate in a periodic unwrapped plate [27], [28]. Therefore, the velocity of helical Lamb wave can be approximately by that of Lamb wave in plate of same thickness. Since Lamb wave owns two type: the symmetric and anti-symmetric modes, the former one of symmetric mode is selected in this work.

III. THEORETICAL MODEL

The Lorentz mechanism is utilized in the proposed EMAT. The magnetic vector potential satisfies the following equation [29].

$$\frac{1}{\mu}\nabla^2 \boldsymbol{A} - \sigma\frac{\partial \boldsymbol{A}}{\partial t} = -\boldsymbol{J_s} \tag{5}$$

where *A* is the magnetic vector potential, μ is the magnetic permeability, σ is the electrical conductivity and J_s is the source current density.

In the skin depth of the material, the eddy current will be induced from the pulse magnetic field. The eddy current can be calculated as

$$\boldsymbol{J_e} = -\sigma\frac{\partial \boldsymbol{A}}{\partial t} \tag{6}$$

where J_e is the induced eddy current density.

Due to the outer static magnetic field from magnets, the Lorentz force will be imposed on the eddy current. The value of Lorentz force depends on the magnetic flux density and the induced eddy current, which is presented as follows:

$$\boldsymbol{F_L} = \boldsymbol{B_0} \times \boldsymbol{J_e} = (\boldsymbol{B_d} + \boldsymbol{B_s}) \times \boldsymbol{J_e} \tag{7}$$

where F_L is the Lorentz force, B_0 is the total magnetic field, B_d is the dynamic magnetic field and *Bs* is the static magnetic field.

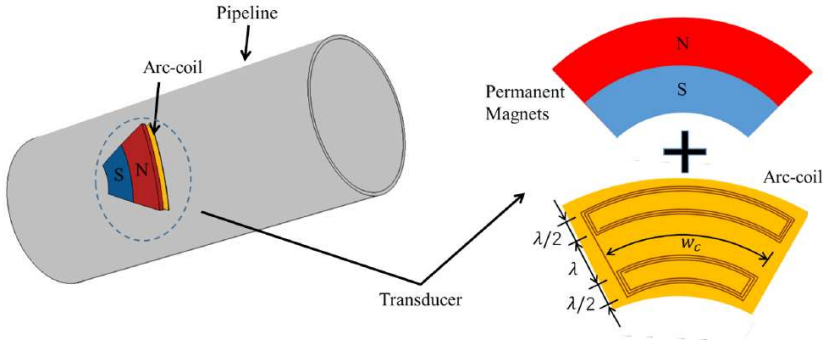

Fig.1 Configuration of the proposed transducer for helical lamb wave and schematic diagrams of the arc-coil. The transducer consists of permanent magnets which is connected to high pulse source, and pipeline itself

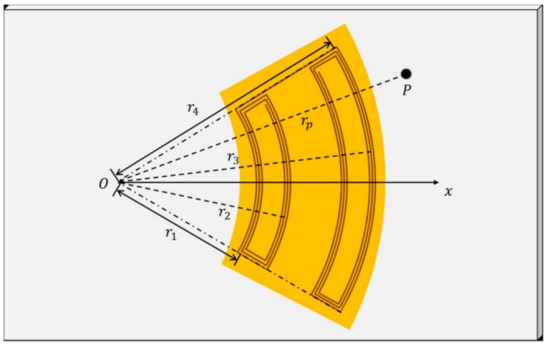

Fig. 2. Illustration of the established coordinates for analyzing working principle of designed arc-coil.

Then the deformation of the material occurs due to the Lorentz force. The material in this case is assumed to be isotropic. The equation of motion can be expressed as

$$\nabla^2 \boldsymbol{u} + (\chi + \kappa)\nabla\nabla \cdot \boldsymbol{u} + \boldsymbol{F_L} = \rho \frac{\partial^2 \boldsymbol{u}}{\partial^2 t^2} \qquad (8)$$

where u is the displacement vector, $\chi$and κ are the Lame Constants, and ρ is material density.

The particle displacement propagates along the structure and forms guided wave. Under the receiver, the vibrations of particles generate dynamic current

$$\boldsymbol{J_v} = \sigma \boldsymbol{v} \times \boldsymbol{B_1} \qquad (9)$$

where $J_v$is the density of dynamic current, v is the particle velocity and B_1 is the static magnetic field from the magnets in the receiver. According to the Faraday law of electromagnetic induction, the coil will generate electromotive force from the dynamic current

$$V = \int_l \boldsymbol{E} \cdot dl = \int_l -\frac{\partial \boldsymbol{A}}{\partial t} \cdot dl \qquad (10)$$

where l is the coil length and E is the electric field generated from the dynamic current. Further, though analyzing the voltage signal sampled from the receiver, the health status of inspected object will be obtained.

IV. Numerical Analysis

The manufacture of transducers brings cost and the corresponding experiment is time-consuming. The numerical analysis based on finite element method provides a cost-efficient way to validate the performance of designed transducers. Since the transduction process of guided wave involves multiple physical fields, COMSOL Multiphysics is adopted to simulate the transducer for helical Lamb wave. The electromagnetic module and solid structure module are used in the model building.

The geometry model is built in the software and the air is also added to form the closed magnetic circuit. The equation of the Lorentz force is entered to the model to obtain the displacement distribution in the pipeline. The components of Lorentz force in the three-dimensional directions are expressed as:

$$\boldsymbol{F_x} = \boldsymbol{J_{ey}} * \boldsymbol{B_z} - \boldsymbol{J_{ez}} * \boldsymbol{B_y} \qquad (11)$$
$$\boldsymbol{F_y} = \boldsymbol{J_{ez}} * \boldsymbol{B_x} - \boldsymbol{J_{xz}} * \boldsymbol{B_z} \qquad (12)$$
$$\boldsymbol{F_z} = \boldsymbol{J_{ex}} * \boldsymbol{B_y} - \boldsymbol{J_{ey}} * \boldsymbol{B_x} \qquad (13)$$

where x, y and z mean the components in three directions. The size of mesh in finite element simulation follows the principle:

$$\Delta x \leq \frac{\lambda}{10} \qquad (14)$$

where Δ_t is the time step and C_L is the velocity of longitudinal wave.

To simulate the actual pipeline, the parameters of corresponding materials are obtained and shown in Table I. The thickness of pipeline is far less than its diameter. Thus, the pipeline can be approximately being considered as flat plate. The parameters of the permanent magnet and pulse are presented in Table II. Under the pipeline thickness of 6 mm and frequency of 130 kHz, the velocity of generated helical wave is 5224.9 m/s through solving the dispersion curve of Lamb wave in plate. Further, the wavelength is 0.040 m and then the sizes of coil can be modeled.

TABLE I
STRUCTURAL AND MATERIAL PARAMETERS OF PIPELINEPE

Name of Parameters	Corresponding Symbol	Value
Outer Diameter	D	273mm
Thickness	h	6mm
Poisson's Ratio	v	0.28
Young's Modulus	E	205 GPa
Density	ρ	7850 kg/m^3
Relative Permeability	μ_{rp}	150
Electrical Conductivity	σ	4.032 x 10^6 S/m
Relative Permeability	ε_r	1

TABLE II
PARAMETERS OF THE HIGH POWER PULSE AND MAGNET

Name of Parameters	Corresponding Symbol	Value
Number of Pulse Cycle	N	5
Pulse Frequency	f_c	130 kHz
Voltage Amplitude	A	200V
Remanent Flux Density	Br	0.3T
Relative Permeability of Magnet	μ_{rm}	1

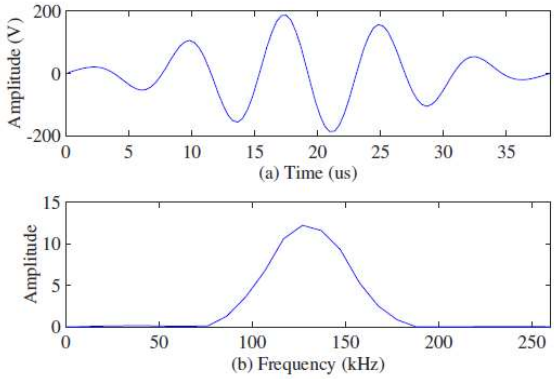

Fig. 3. The tone-burst is chosen as the excitation signal. It is essentially the windowed sinusoidal signal.

parameters of the permanent magnet and pulse are presented in Table II. Under the pipeline thickness of 6 mm and frequency of 130 kHz, the velocity of generated helical wave is 5224.9 m/s through solving the dispersion curve of Lamb wave in plate. Further, the wavelength is 0.040 m and then the sizes of coil can be modeled.

The magnetic field is first analyzed. The waveform of pulse and its spectrum are depicted in Fig. 3. The pulse has a total time duration of 38.5 μs and its spectrum owns a better main-lobe characteristic due to the added Hamming window. According to the Maxwell's equations, the static magnetic field from the magnet and the dynamic magnetic field from the coil can be calculated by finite element method. The results are shown in Fig. 4.

As Fig. 4(a) indicates, the maximum static magnetic field in the pipe is around 0.2 T. The distribution of magnetic field is relatively uniform and the strength is mainly focused on the nearby region. From Fig. 4(b), it suggests that the dynamic magnet field generated from the pulse is relatively small and it is concentrated on the region under the coil. Because the pulse forms alternating current in the coil, the dynamic magnet field is also alternating. After the interaction with the steel material of pipeline, the eddy current is also generated. Under the static magnetic field, the eddy current will be influenced by Lorentz force and the results are depicted in Fig. 5. The time transient analysis is applied and two time nodes are chosen to observe the Lorentz force.

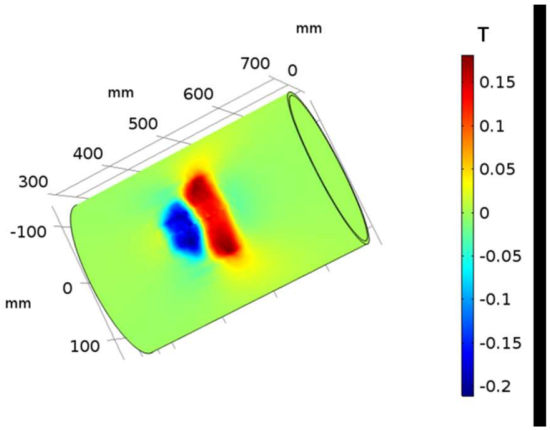

(a) The static magnetic field from the permanent magnets

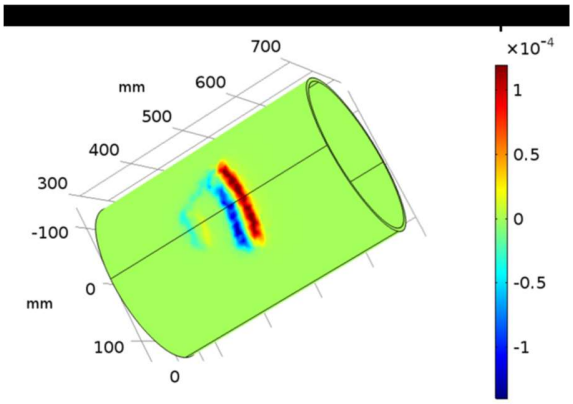

(b) The dynamic magnetic field from the coil at 1.76 μs

Fig. 4. The distribution of magnetic field in the designed transducer.

As Fig. 5 shows, the directions of the force are different with each other in the two time nodes, which is in coherent with the variation of excitation pulse. Thus, the Lorentz force is alternating and this causes the vibration of particles. The vibration can propagate along the structure and generate helical guided wave. To study the propagation of guided wave, the displacement distribution in the circumferential direction called angular profile is presented in different propagation distances. The 0 (also 360) is defined as the angle position ahead of the transmitter. Three positions are chosen to observe the propagation process. The results of angular profiles are depicted in Fig. 6. It is shown that with the wave spreading forward, the beam becomes disperse but the main energy is concentrated in a certain range of angle. The simulation demonstrates that the guided wave can not only propagate in the angle along the axial direction, but also can spread in spiral direction along the helical curve of pipe structure. Therefore, the transducer can generate helical Lamb wave with concentrated beam, which is advantageous to enhance the energy in the inspected region.

(a) The generated Lorentz force at 9.5 μs

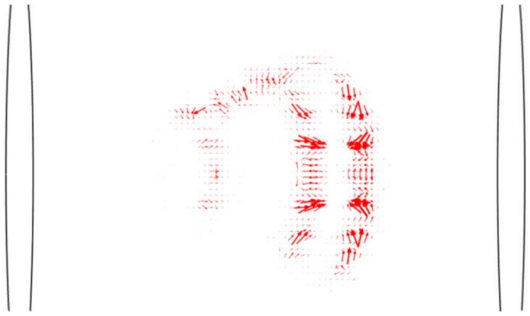

(b) The generated Lorentz force at 13.5 μs

Fig. 5. Under the magnetic field, the eddy current is influenced by Lorentz force.

V. Experiments and Further Discussion

A. Experimental Setup and Procedure

The pipeline inspection platform is established to verify the performance of developed transducer. The schematic diagram is presented in Fig. 7. The transducers are customized according to the designed parameters calculated from the wavelength and pipeline dimensions. The transmitter is fixed on the left of pipeline. The length, thickness and outer diameter are 3000, 6 and 273 mm, respectively. The pulse is generated by arbitrary waveform generator and then amplified by power amplifier (RITEC RPR-4000). The impedance matching pad is connected between the amplifier and transmitter to increase the efficiency. The receiver is also connected to RITEC RPR- 4000 which owns the broadband receiver. The parameters for the pulse are the same as those set in the simulation. The waveform can be observed in the oscilloscope and the data is transferred to laptop to further analyze the results.

The transmitter maintains in one position in the experiments. The receiver is moved along the circumferential direction in the outside of pipeline to receive the generated helical Lamb wave. Eight positions evenly distributed with angular difference of 45° are selected. Through varying the position of receiver, the distribution of helical Lamb wave signal can be obtained. Subsequently, the results can be compared with those in the simulation.

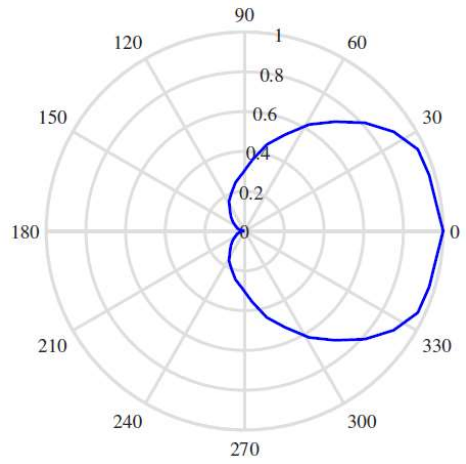

(a) The angular profile at position 200 mm

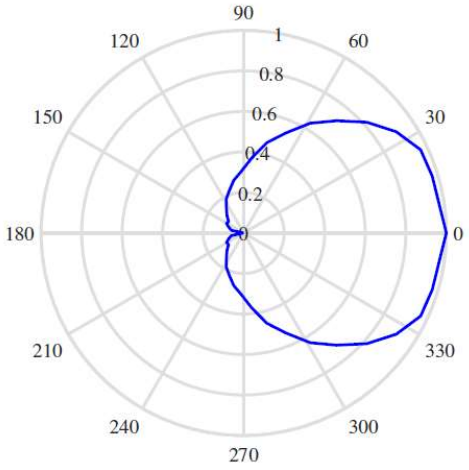

(b) The angular profile at position 250 mm

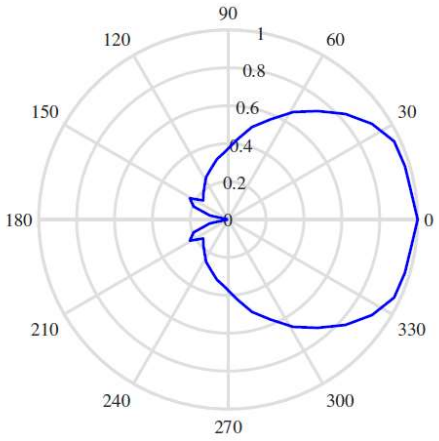

(c) The angular profile at position 300 mm

Fig. 6. The angular profile of wave propagating along the pipe in the simulation. The angular profile is the displacement distribution in the circumferential direction.

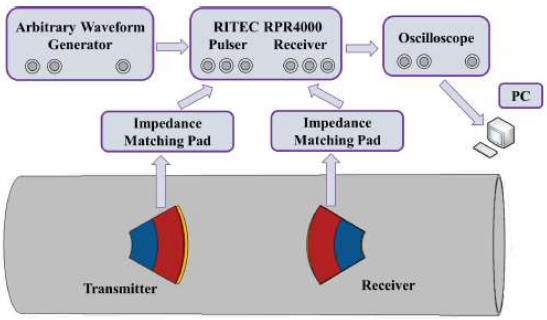

Fig. 7. Experimental setup for verification of the developed helical Lamb wave transducer.

TABLE III
THE WAVE VOELOCITIES AT THREE AUNGULAR POSITIONS

Angular Positions	Time-of-flight (μs)	Velocity (m/s)	Relative Error
0°	57.3	5235.6	0.20%
45°	61.2	5212.4	0.24%
315°	61.3	5203.9	0.4%

B. Results of Guided Wave Generation and Reception

The waveform from receiver at three angular positions with an axial distance of 300 mm are depicted in Fig. 8. It is observed that the helical Lamb wave arrives earliest at 0 where the wave propagates in direct way. The arrival times of wave at 45° and 315° are nearly the same. Therefore, the generated wave owns a certain range of angle and propagates spirally around the pipe. Because the wave velocity is vital parameter when identifying the defect location and further imaging, the velocity of helical Lamb wave is also calculated to verify it is whether or not consistent with the theoretical value. The time-of-fight is defined as the time difference between excitation time and arrival time. In the three chosen positions, the time-of-fights are obtained and corresponding velocities are given in Table III. The equation to calculate the relative error can be expressed as follows:

$$R_e = \frac{|V_{ac} - V_{th}|}{V_{th}} \qquad (16)$$

where *Re* is the relative error, *Vth* is the theoretical velocity of Lamb wave in plate of same thickness and *Vac* is the obtained wave velocity in experiments. According to Table III, the relative error is less than 0:5%. Thus, the results suggest that the velocity of helical Lamb wave is similar to that of Lamb wave in plate.

To present the distribution of wave in the circumferential direction of pipeline, the angular profile of signal amplitude is illustrated in Fig. 9. The dots mean the value in the experiment and the solid line is obtained in aforementioned simulation. The results validate that the acoustic beam has a main beam due to the fan-shaped transducer. Thus the energy is relatively concentrated compared with omni-directional transducer. Meanwhile, the generated wave distributes in a certain range of angle to form helical Lamb wave. Then the helical wave can propagate through the inspected region with different angles and the receiver can gain more information about the health status.

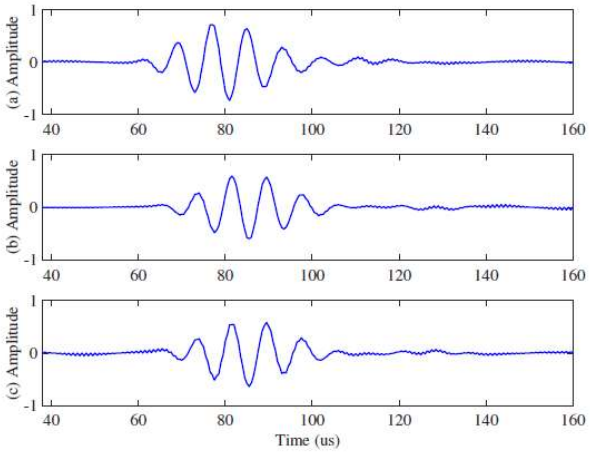

Fig. 8. The waveform receiver at three angular positions along the circumferential direction of pipeline. (a) angular position of 0° (b) 45° (c) 315°

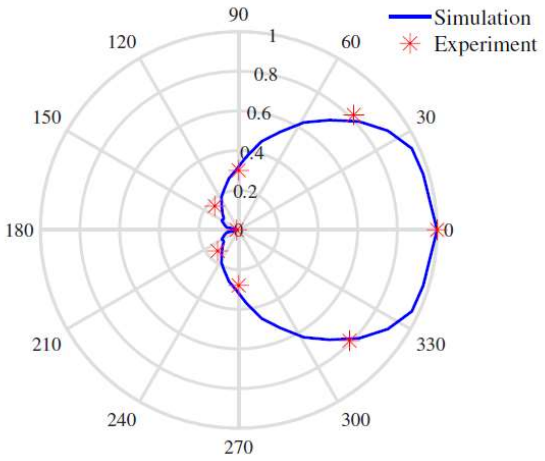

Fig. 9. The angular profile of signal amplitude distributed in the circumferential direction.

C Comparison with Traditional Transducer

To verify the superiority of the proposed transducer, the comparison with traditional transducer is conducted. The common used transducer is composed of permanent magnet and meander coil. The coil is shown in Fig. 10. The distance between the two adjacent coils matches the wavelength to utilize the superposition which can enhance the signal-to-noise ratio. The width is denoted as *wc*. The magnet owns the same shape with the coil and is placed above it to provide static magnetic field.

It is worth noting that both the transducers need the custom manufacture for different frequencies and pipe dimensions.

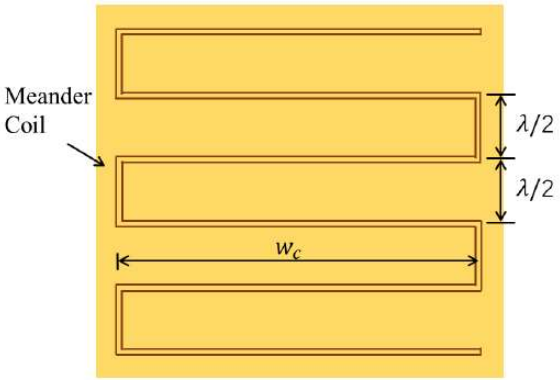

Fig. 10. The traditional transducer uses meander coil. The coil is shown and its parameter matches the wavelength.

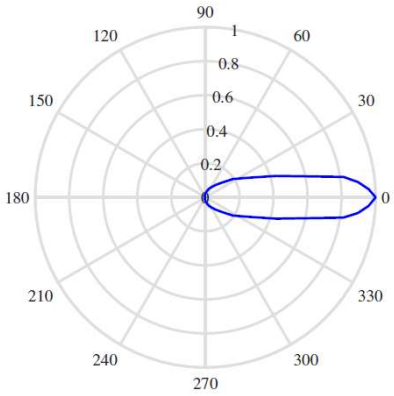

Fig. 11. The obtained angular profile at position 300 mm using the traditional transducer.

The cost in making the transducer includes the PCB fabrication and the magnet machining. The cost difference between the designed transducer and traditional transducer is mainly dependent on the magnet machining. Due to adaptive shape of the magnets in the proposed transducer, it is more expensive than the traditional transducer.

The traditional transducer is excited with same tone-burst to generate helical Lamb wave. The obtained angular profile at 300 mm is presented in Fig. 11. It can be seen that the guided wave is mainly concentrated in the direction ahead the transducer. It has a narrower beam than that of the developed transducer. Therefore, the structure is not advantageous to generate helical wave.

The propagation distance of generated wave is tested for these two transducers. The receiver is placed in the longer axial distance to evaluation the propagation capacity. With the increase of the propagation distance, the signal-noise ratio becomes lower. Under the same excitation signal, the longest distances where the wave can be detected are 6.7 and 9.5 m for the proposed transducer and traditional transducer, respectively. The tradition transducer is advantageous in the propagation distance because of its focused beam.

The radiation beam profile is also studied to further analyze the performance of transducers. The half-angle of divergence is proposed in plate to help design the rotation angle of transducers [30]. Its illustration is shown in Fig. 12. This concept is extended to pipe-like structure and its definition is expressed as follows:

$$\tan\theta = \frac{l_h}{d_p} \qquad (17)$$

where θ is the half-angle of divergence, l_h is the half of the circumferential length where the beam is concentrated and dp is axial distance in pipeline.

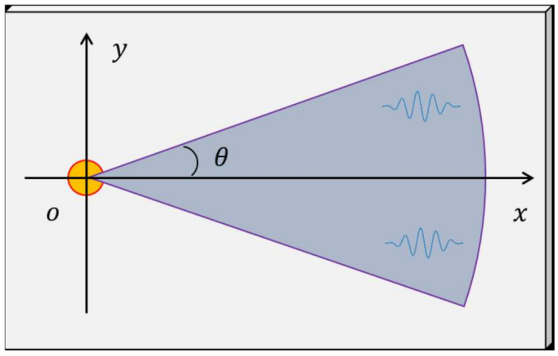

Fig.12. The illustration of the half-angle of divergence to depict the radiation beam profile.

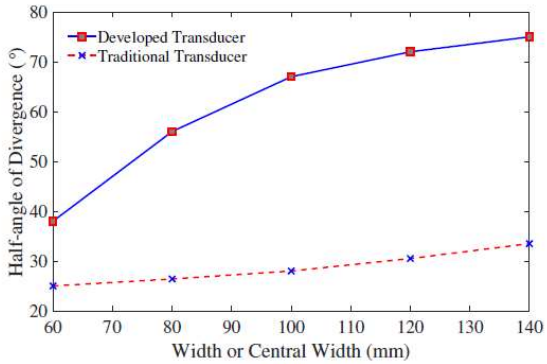

Fig.13. The comparison of the half-angle of divergence from the developed transducer and traditional transducer.

Due to the coil width owns important influence in the generated guided wave, the widths of the coils are set as the same value to obtain the effective comparison of the two transducers. In this work, five different sizes of coils are chosen to verify the performance. The magnet will be modified as the coil changes. In order to eliminate the interference, the excitation pulse and other factors keep the same parameters in the experiments. The results of the calculated half-angle of divergence are shown in Fig. 13. It clearly shows that with the increase of the coil width, the half-angle of divergence increases in both transducers. Therefore, the coil width greatly affects the characteristics of beam profile. It can also be seen that the developed transducer owns larger half-angle of divergence than the traditional transducer significantly in five different sizes. Furthermore, the relation between the half angle

of divergence and width is not linear. The slope of the curve for traditional transducer becomes larger when the width increases, while the curve for designed transducer is in the opposite situation. However, the gap of half-angle of divergence between the two transducers is still large. Therefore, according to the comparison and analysis, the proposed transducer is more suitable to generate guided wave with helical angle.

VI. Conclusion and Future Work

In this article, a novel design of transducer for helical Lamb wave is proposed for pipeline inspection. The transducer is composed of permanent magnets and arc-coil. The structural parameters of the arc-coil is deliberately designed to match the wavelength and enhance the signal strength. The theoretical model is constructed using the mechanism of Lorentz force and it is verified by numerical simulation. The angular profiles of different propagation distances indicate that the generated guided wave mainly distributed in a certain range of angle. The established experimental system is used successfully to generate helical Lamb wave and the angular profile agrees with that from the simulation. The half-angle of divergence is adopted to analyze the performance. Compared with traditional transducer, the transducer presented here allows larger halfangle of divergence. The parameter of central width can introduce significant differences to the divergence and it should be considered when applying in specific case. As a consequence, the developed transducer is effective in generating helical guided wave for pipeline inspection. In the future work, the interaction of wave with defect needs to be investigated to help pave the way of actual application of helical Lamb wave.

References

[1] M. J. S. Lowe, D. N. Alleyne, and P. Cawley, "Defect detection in pipes using guided waves," Ultrasonics, vol. 36, no. 1-5, pp. 147–154, 1998.

[2] A. Ghavamian, F. Mustapha, B. T. Baharudin, and N. Yidris, "Detection, localisation and assessment of defects in pipes using guided wave techniques: A review," Sensors, vol. 18, no. 12, p. 4470, 2018.

[3] J. He, C. Zhou, L. Yang, and X. Sun, "Research on pipeline damage imaging technology based on ultrasonic guided waves," Shock and Vibration, vol. 2019, 2019.

[4] P. Tse, Z. Fang, and K. Ng, "Novel design of a smart and harmonized flexible printed coil sensor to enhance the ability to detect defects in pipes," NDT & E International, vol. 103, pp. 48–61, 2019.

[5] F. Yan, R. L. Royer, and J. L. Rose, "Ultrasonic guided wave imaging techniques in structural health monitoring," Journal of Intelligent Material Systems & Structures, vol. 21, no. 3, pp. 377–384, 2010.

[6] Z. Wei, S. Huang, S. Wang, and W. Zhao, "Magnetostriction-based omni-directional guided wave transducer for high-accuracy tomography of steel plate defects," IEEE Sensors Journal, vol. 15, no. 11, pp. 6549–6558, 2015.

[7] M. Mitra and S. Gopalakrishnan, "Guided wave based structural health monitoring: A review," Smart Materials and Structures, vol. 25, no. 5, p. 53001, 2016.

[8] C. Su, M. Jiang, J. Liang, A. Tian, L. Sun, L. Zhang, F. Zhang, and Q. Sui, "Damage identification in composites based on hilbert energy spectrum and lamb wave tomography algorithm," IEEE Sensors Journal, vol. , no. , pp. 1–1, 2019.

[9] I. K. Kim and Y. Y. Kim, "Wireless frequency-tuned generation and measurement of torsional waves using magnetostrictive nickel gratings in cylinders," Sensors and Actuators A: Physical, vol. 126, no. 1, pp. 73–77, 2006.

[10] E. Kannan, B. W. Maxfield, and K. Balasubramaniam, "SHM of pipes using torsional waves generated by in situ magnetostrictive tapes," Smart Materials and Structures, vol. 16, no. 6, pp. 2505–2515, 2007.

[11] F. Li, H. Peng, and G. Meng, "Quantitative damage image construction in plate structures using a circular pzt array and lamb waves," Sensors and Actuators A: Physical, vol. 214, pp. 66 – 73, 2014.

[12] S. Wang, S. Huang, Y. Zhang, and W. Zhao, "Multiphysics modeling of a lorentz force-based meander coil electromagnetic acoustic transducer via steady-state and transient analyses," IEEE Sensors Journal, vol. 16, no. 17, pp. 6641–6651, 2016.

[13] N. Lunn, S. Dixon, and M. Potter, "High temperature emat design for scanning or fixed point operation on magnetite coated steel," NDT & E International, vol. 89, pp. 74–80, 2017.

[14] M. Gori, S. Giamboni, E. D'Alessio, S. Ghia, F. Cernuschi, and G. M. Piana, "Guided waves by emat transducers for rapid defect location on heat exchanger and boiler tubes," Ultrasonics, vol. 34, no. 2-5, pp. 311– 314, 1996.

[15] C. L. Willey, F. Simonetti, P. B. Nagy, and G. Instanes, "Guided wave tomography of pipes with high-order helical modes," NDT & E International, vol. 65, pp. 8–21, 2014.

[16] P. Huthwaite and M. Seher, "Robust helical path separation for thickness mapping of pipes by guided wave tomography," IEEE Transactions on Ultrasonics, Ferroelectrics, and Frequency Control, vol. 62, no. 5, pp. 927–938, 2015.

[17] H. W. Kim, H. J. Lee, and Y. Y. Kim, "Health monitoring of axiallycracked pipes by using helically propagating shear-horizontal waves," NDT & E International, vol. 46, pp. 115–121, 2012.

[18] H. Kwun, J. J. Hanley, and A. E. Holt, "Detection of corrosion in pipe using the magnetostrictive sensor technique," in Nondestructive Evaluation of Aging Infrastructure. International Society for Optics and Photonics, 1995, pp. 140–148.

[19] Z. Liu, Y. Hu, J. Fan, W. Yin, X. Liu, C. He, and B. Wu, "Longitudinal mode magnetostrictive patch transducer array employing a multisplitting meander coil for pipe inspection," NDT & E International, vol. 79, pp. 30–37, 2016.

[20] S. H. Cho, C. I. Park, and Y. Y. Kim, "Effects of the orientation of magnetostrictive nickel strip on torsional wave transduction efficiency of cylindrical waveguides," Applied Physics Letters, vol. 86, no. 24, p. 244101, 2005, identifier: 10.1063/1.1948534.

[21] Nurmalia, N. Nakamura, H. Ogi, and M. Hirao, "Mode conversion and total reflection of torsional waves for pipe inspection," Japanese Journal of Applied Physics, vol. 52, no. 7, 2013.
[22] X. Zhao, V. K. Varma, G. Mei, B. Ayhan, and C. Kwan, "In-line nondestructive inspection of mechanical dents on pipelines with guided shear horizontal wave electromagnetic acoustic transducers," Journal of pressure vessel technology, vol. 127, no. 3, pp. 304–309, 2005.
[23] K. R. Leonard and M. K. Hinders, "Guided wave helical ultrasonic tomography of pipes," The Journal of the Acoustical Society of America, vol. 114, no. 2, pp. 767–774, 2003.
[24] Z. Wang, S. Huang, S. Wang, Q. Wang, and W. Zhao, "Development of a new emat for multi-helical sh guided waves based on magnetostrictive effect," in 2018 IEEE International Instrumentation and Measurement Technology Conference (I2MTC). IEEE, 2018, pp. 1–6.
[25] K. R. Leonard and M. K. Hinders, "Lamb wave tomography of pipe-like structures," Ultrasonics, vol. 43, no. 7, pp. 574–583, 2005.
[26] H. W. Kim, J. K. Lee, and Y. Y. Kim, "Shear-horizontal wave-based pipe damage inspection by arrays of segmented magnetostrictive patches," IEEE Transactions on Ultrasonics Ferroelectrics and Frequency Control, 2011.
[27] J. Li and J. L. Rose, "Natural beam focusing of non-axisymmetric guided waves in large-diameter pipes," Ultrasonics, vol. 44, no. 1, pp. 35–45, 2006.
[28] A. Velichko and P. D. Wilcox, "Excitation and scattering of guided waves: Relationships between solutions for plates and pipes," The Journal of the Acoustical Society of America, vol. 125, no. 6, pp. 3623– 3631, 2009.
[29] K. Hao, S. Huang, W. Zhao, S. Wang, and J. Dong, "Analytical modelling and calculation of pulsed magnetic field and input impedance for emats with planar spiral coils," NDT & E International, vol. 44, no. 3, pp. 274–280, 2011.
[30] S. Advani, J. Van Velsor, and J. L. Rose, "Beam divergence calculation of an electromagnetic acoustic transducer for the non-destructive evaluation of plate-like structures," in 2011 IEEE Sensors Applications Symposium, 2011, pp. 277–282.M. Hirao and H. Ogi, "An SH-wave EMAT technique for gas pipeline inspection," *NDT & E Int.*, vol. 32, no. 3, pp. 127–132, Apr. 1999.

Zhe Wang received a B.S. degree from School of Electrical Engineering, Chongqing University, Chongqing, China in2016. He is currently pursuing a Ph.D. degree within the Department of Electrical Engineering, Tsinghua University, Beijing, China. His current research interests include electromagnetic measurement and nondestructive evaluation.

Songling Huang received a bachelor's degree in automatic control engineering from Southeast University, Nanjing, China, in 1991, and a Ph.D. degree in nuclear application technology from Tsinghua University, Beijing, China, in 2001. He is currently a Professor within the Department of Electrical Engineering, Tsinghua University. His research interests include nondestructive evaluation and instrument techniques.

Shen Wang received the bachelor's and Ph.D. degrees in electrical engineering from Tsinghua University, Beijing, China, in 2002 and 2008, respectively. He is currently a Research Assistant with the Department of Electrical Engineering, Tsinghua University. His research interests include nondestructive testing and evaluation, and virtual instrumentation.

Qing Wang received the B.Eng. degree in electronic instrument and measurement technique from Beihang University, Beijing, China, in 1995, the M.Sc. degree in advanced manufacturing and materials from the University of Hull, Hull, U.K., in 1998, and the Ph.D. degree in manufacturing management from De Montfort University, Leicester, U.K., in 2001. She is currently an Associate Professor with the School of Engineering and Computing Sciences, Durham University, Durham, U.K. Her research interests include electronic instruments and measurement, computer simulation, and advanced manufacturing technology.

Wei Zhao received the bachelor's degree in electrical engineering from Tsinghua University, Beijing, China, in 1982, and the Ph.D. degree from the Moscow Power Engineering Institute Technical University, Moscow, Russia, in 1991. He is currently a Professor with the Department of Electrical Engineering, Tsinghua University. His research interests include modern electromagnetic measurement and instrument techniques.